NASA TECHNICAL MEMORANDUM

NASA TM X-1837

NASA TM X-1837

EXPERIMENTAL LATERAL BENDING DYNAMICS OF THE ATLAS-CENTAUR-SURVEYOR LAUNCH VEHICLE

by Robert P. Miller and Theodore F. Gerus

Lewis Research Center
Cleveland, Ohio

NATIONAL AERONAUTICS AND SPACE ADMINISTRATION • WASHINGTON, D. C. • JULY 1969

NASA TM X-1837

EXPERIMENTAL LATERAL BENDING DYNAMICS OF THE ATLAS-CENTAUR-SURVEYOR LAUNCH VEHICLE

By Robert P. Miller and Theodore F. Gerus

Lewis Research Center
Cleveland, Ohio

NATIONAL AERONAUTICS AND SPACE ADMINISTRATION

For sale by the Clearinghouse for Federal Scientific and Technical Information
Springfield, Virginia 22151 – CFSTI price $3.00

ABSTRACT

A series of full-scale dynamic tests was conducted to determine the lateral bending dynamics of the Atlas-Centaur-Surveyor launch vehicle. The tests were made at several simulated flight times to obtain a good experimental definition of the vehicle dynamic response in the bending mode frequency range. Parameters measured were bending mode frequencies, damping, mode shapes, and linearity. The bending mode frequencies measured ranged from 2.59 to 31.9 Hz. Damping measured averaged about 2.0 percent of critical. Mode shapes were well defined and continuous in the lower-frequency modes but indicated discontinuities in the higher modes. The modal response was very linear over the excitation range chosen, and only small differences between pitch and yaw axes were seen Phase relations of various response points for three modes were also measured.

EXPERIMENTAL LATERAL BENDING DYNAMICS OF THE ATLAS-CENTAUR-SURVEYOR LAUNCH VEHICLE

by Robert P. Miller and Theodore F. Gerus

Lewis Research Center

SUMMARY

A series of full-scale dynamic tests was conducted to determine the lateral bending dynamics of the Atlas-Centaur-Surveyor launch vehicle. The tests were made at several simulated flight times to obtain a good experimental definition of the vehicle dynamic response in the bending mode frequency range. Parameters measured were bending mode frequencies, damping, mode shapes, and linearity.

The bending mode frequencies measured ranged from 2.59 to 31.9 hertz. Damping measured averaged about 2.0 percent of critical. Mode shapes were well defined and continuous in the lower-frequency modes but indicated discontinuities in the higher modes. The modal response was very linear over the excitation range chosen, and only small differences between pitch and yaw axes were seen. Phase relations of various response points for three modes were also measured.

INTRODUCTION

The design of the Atlas-Centaur launch vehicle has evolved as a relatively long, thin-walled pressurized cylinder (fig. 1). The control of this structure in flight results in the interaction of the vehicle lateral bending modes with the flight control system. Such coupling exists because the control system attitude sensors detect angular position and rates caused by structural deformations. In the case of the Atlas-Centaur, the lower-frequency bending modes are within the control system response range for a large portion of powered flight. The stability of the vehicle control, therefore, requires examination of the corresponding closed-loop modes of the vehicle structure and the control system. A schematic of the control system is shown at the top of the next page.

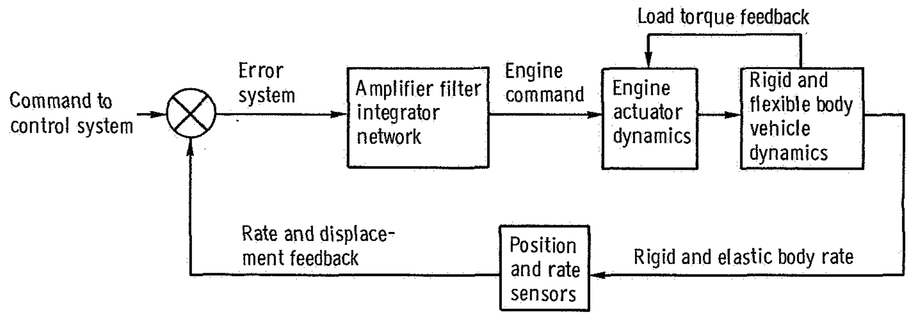

It was the purpose of the lateral dynamics tests to experimentally determine the frequencies, mode shapes, and damping characteristics of the Atlas-Centaur-Surveyor at various simulated flight times in order that accurate elastic modal data could be incorporated in the elastic stability analysis as well as in the analysis for loads and clearance. The complexity of the Atlas-Centaur structure, with its many discontinuities and branches, makes analytical predictions difficult. A test of the lateral bending dynamics of the vehicle was made to improve the analysis techniques and/or to gain confidence in these techniques.

APPARATUS AND PROCEDURE

The tests were conducted on a full-scale, production-type Atlas-Centaur vehicle and a dynamic model of the Surveyor spacecraft. The vehicle was suspended on soft springs to simulate the free-free condition of flight and excited laterally at the gimbal plane with an electrodynamic shaker. Natural frequencies, mode shapes, and damping characteristics of the vehicle were studied. The mass distribution of the propellants was approximated with water in the Atlas liquid-oxygen and fuel tanks and the Centaur liquid-oxygen tank. Polystyrene balls were used to simulate the mass of the liquid-hydrogen fuel in Centaur.

Test Setup

All testing described herein was accomplished at the E site of Plum Brook Station. The E site consists of a 140-foot- (42.6-m-) high steel tower designed to accommodate the

Atlas-Centaur vehicle (see fig. 2).

The test vehicle consisted of a complete Atlas-Centaur launch vehicle including nose fairing and Centaur insulation panels. A dynamic model of the Surveyor spacecraft was used in all tests. To facilitate mating with the suspension system, the Atlas was modified by replacing all structure and components aft of the thrust barrel with an equivalent mass beam structure X-frame (see fig. 2). The bending and shear stiffnesses of the vehicle are given in figures 3 and 4 and the mass distribution of the empty vehicle is given in figure 5.

A suspender consisting of a steel cable, a spring box, a hydraulic cylinder, and a load cell was fastened to each of the four frame ends (fig. 2). Each spring box contained 4 to 16 springs with a constant of about 400 pounds per inch (7.0×10^4 N/m) per spring. The number of springs for each test was proportioned to the vehicle weight for the particular configuration to give a static deflection of approximately 1 foot (0.3 m), keeping the natural rocking frequency of the suspension system an order of magnitude below the first bending mode frequency of the vehicle. Lateral stability of the system was provided at the bottom by the $1/2^{\circ}$ (8.7×10^{-3} rad) inclination of the cables and at the top by horizontal springs (fig. 2). The test setup was similar to that used in the longitudinal dynamics tests in reference 1.

To avoid operational problems involved with the handling of cryogenic propellants, an equal volume of deionized water was used instead of liquid oxygen and RP fuel. Polystyrene balls having an equivalent bulk density replaced the liquid hydrogen. With the exception of the first test, the propellant tanks were maintained at flight pressures of 31.0 and 59 psig (21.3×10^4 and 40.6×10^4 N/m^2 gage) in the Atlas liquid-oxygen and fuel tanks, respectively, and 15 and 5 psig (10.3×10^4 and 3.44×10^4 N/m^2 gage) in the Centaur liquid-oxygen and liquid-hydrogen tanks, respectively.

The tank pressures for the first test were maintained at the standby conditions of 17 psig (11.7×10^4 N/m^2) in the Atlas fuel tank, 10 psig (6.89×10^4 N/m^2) in the Atlas liquid-oxygen tank, 10 psig (6.89×10^4 N/m^2) in the Centaur liquid-oxygen tank, and 5 psig (3.44×10^4 N/m^2) in the Centaur fuel tank. The weight and levels of the simulated propellants are given in table I, along with tank pressures used during the tests.

Instrumentation

Instrumentation for all tests consisted of strain-gage-type accelerometers. Locations on the X-axis and Y-axis sides are shown in figure 6. The accelerometers sensed acceleration perpendicular to the longitudinal (Z) axis of the vehicle. In the area of the Centaur insulation panels, holes were cut in the panels to allow attachment of the accelerometers to the tank skin. Load cells were used for both vehicle weighing and measurement of the driving force. All modal data were digitally recorded and reduced with a digital computer program. Sixteen channels of data were recorded on oscillograph paper. All damping was determined by the logarithmic decay method from the analog traces on oscillograph paper. End-to-end system accuracy of the instruments is considered to be approximately 2 percent of full scale. Full-scale ranges of instruments were as follows:

Accelerometers, g (m/sec^2) . . . . ±1.0 (±9.8)
Load cell (force), lb (N) . . . . ±1000 (±4.45×10^3)

Test Procedure

The vehicle tanks (except for the Centaur hydrogen tank) were filled with water and pressurized to simulate the flight conditions as presented in table I. Excitation was then applied to the suspended vehicle by an electrodynamic shaker through a load cell and the X-frame at frequencies varying from 1 to 40 hertz. Input force levels ranged from 30 to 400 pounds (133 to 1779 N).

Inasmuch as a tank rupture hazard existed at the tank pressures used, it was necessary to control all operations remotely once the tanking procedures were begun. These remote operations were conducted from a control room (H-building) located approximately 1/4 mile (400 m) away. Television cameras were used to visually monitor the vehicle.

The resonant frequencies of the vehicle were determined by slowly increasing the excitation frequency while holding the force input constant. Resonance was established when acceleration at the extremities of the vehicle peaked.

When resonant conditions were determined, transducer output was recorded on analog recorders and on digital tape. At the resonance peak, the shaker was electrically decoupled allowing natural decay of the oscillations, with the transducer output being recorded on the analog recorder. This procedure was followed to identify modes for each tanking condition.

RESULTS AND DISCUSSIONS

The test results are discussed in terms of the following major subjects:

(1) Natural frequencies

(2) Mode shapes

(3) Damping

(4) Linearity of response

(5) Phase relations of various parts of the mode

Natural Frequencies

Figure 7 illustrates the variation of natural frequency of each mode with the simulated propellant level associated with vehicle flight times. The variation is shown only for the pitch (Y-Z) plane. Tables II lists natural frequencies as a function of flight time, plane of excitation, and pressure level. It is noted that although tank pods exist in the pitch plane and not in the yaw plane, the effect on natural frequency is minor. Further, two tests run at significantly different pressures show little variation in natural frequency. This is probably due to the linearity of this structure as is discussed later.

Mode Shapes

Mode shapes measured at each of the natural frequencies are plotted in figures 8(a) to (i). The mode shapes are shown for both the pitch (Y-Z) and yaw (X-Z) planes and for two tank pressures for the empty vehicle configurations. Although mode shapes are easily defined as clean, continuous curves in the lower-frequency modes, the higher-frequency modal curves show breaks in the smoothness of the mode shape. A comparison of mode shapes in the two planes indicates that although lower modes compare reasonably, higher modes are significantly different in shape. The shapes of the first two modes in the pitch (Y-Z) plane at two significantly different tank pressures compare reasonably well, as demonstrated by figures 8(b) and (c).

Damping

One of the most difficult parameters to measure in a test of this nature is damping. Even though every effort was made in the design and operation of the test setup to assure that no damping was introduced through the manner in which the vehicle was suspended, no quantitative measure of test-stand-introduced damping was possible. The typical decays shown in figure 9 present an example of the data from which damping was derived. Damping was determined by the logarithmic decay method (ref. 2). A plot of the damping variation with flight time in the Y-Z plane (pitch) is shown in figure 10. A typical value of damping in the pitch plane obtained from flight data during the booster engine cutoff (BECO) transient (T + 150 sec) is also plotted in figure 10. A damping value of 3 percent obtained from flight data compares to 2.2 percent measured in testing at this same simulated flight time.

Linearity of Response

One of the more significant problems associated with analysis of control systems and loads interacting with the flexible-body bending modes is the linearity of these modes. Nonlinearities in modal response relative to forcing function level could dictate either convergence or divergence of loads or autopilot stability. Responses of the first four bending modes as a function of force level are shown in figure 11. The data shown in figure 11 indicate the modal response is linear for each of the modes over the excitation range chosen.

Phase Relations of Various Parts of Mode

It is necessary to measure angular position and rate at a number of positions on a typical launch vehicle in order to provide the right amplitude and phase of bending mode relations in the autopilot. In the analysis of these control systems, orthogonal modes are assumed; that is, phase relations between any two parts of a vehicle are assumed to be either 0° or 180° for any vehicle mode, depending on the shape of the bending mode. To evaluate the limitations of this analysis technique, phase relations between force and acceleration were measured for frequencies near each of the first three bending modes. Figure 12 indicates the amount of phase differences associated with each of these frequencies. As the figure shows, very little deviation from orthogonality occurs in the first two modes. However, the third mode indicates significant differences in phase relations.

CONCLUSIONS

Based on the results of the lateral dynamics tests of the Atlas-Centaur-Surveyor vehicle, the following conclusions are drawn:

1. The natural bending mode frequency is only slightly affected by tank pressure.
2. The bending mode frequency is essentially the same for excitation of the vehicle in the XZ and YZ planes.
3. The mode shapes for the first two modes are well defined, while the higher modes become less well defined.
4. Damping of the vehicle averaged about 2 percent of critical.
5. Modal response is indicated to be linear for each of the modes over the excitation range.

6. Very little deviation from orthogonality is indicated in the first two modes. The third and higher modes indicate significant deviation in phase relations.

Lewis Research Center,
National Aeronautics and Space Administration,
Cleveland, Ohio, April 8, 1969,
491-05-00-03-22.

REFERENCES

1. Gerus, Theodore F.; Housely, John A.; and Kusic, George: Atlas-Centaur-Surveyor Longitudinal Dynamics Tests. NASA TM X-1459, 1967.
2. Harris, Cyril M.; and Crede, Charles E.: Shock and Vibration Handbook. Vol. 1. McGraw-Hill Book Co., Inc., 1961.

TABLE I. - TEST CONDITIONS

Test configuration	Units	Test number and simulated flight time					
		I	II and VII	III and VIII	IV	V and IX	VI and X
		Tanks empty	Tanks empty	T + 150 (max. g)	T + 100	T + 75 (max. αQ)	T + 0 (lift-off)
Atlas fuel tank							
Weight of water	lb N	0 0	0 0	10 050 44 600	38 500 171 000	51 000 226 000	93 000 412 000
Water level	Station	0	0	1144	1077	1077	940
Tank pressure	psig N/m^2	17 11.68×10^4	59 40.5×10^4	59 40.5×10^4	59 40.5×10^4	59 40.5×10^4	59 40.5×10^4
Atlas liquid-oxygen tank							
Weight of water	lb N	0 0	0 0	14 600 64 700	58 300 258 200	81 200 360 000	150 000 665 000
Water level	Station	0	0	895	786	734	556
Tank pressure	psig N/m^2	10.0 6.86×10^4	31.0 21.25×10^4	31.0 21.25×10^4	31.0 21.25×10^4	31.0 21.25×10^4	31.0 21.25×10^4
Centaur liquid-oxygen tank[a]							
Weight of water	lb N	0 0	0 0	21 400 95 000	21 400 95 000	21 400 95 000	21 400 95 000
Water level	Station	0	0	382	382	382	382
Tank pressure	psig N/m^2	10.3 6.86×10^4	15.0 10.3×10^4	15.0 10.3×10^4	15.0 10.3×10^4	15.0 10.3×10^4	15.0 10.3×10^4
Total weight (including weight of tanks)	lb N	25 530 113 200	25 530 113 200	71 580 318 000	143 730 636 000	179 130 795 000	289 930 1 285 000

[a]Conditions of Centaur liquid-hydrogen tank were the same for all tests: weight of polystyrene, 4630 pounds (20 500 N); level of polystyrene, station 209; tank pressure, 5.0 psig (3.43×10^4 N/m^2).

TABLE II. - EXPERIMENTAL NATURAL FREQUENCIES AND DAMPING RATIOS FOR TEST SIMULATED FLIGHT CONDITIONS

(a) Excitation force in Y-Z plane

Test condition	Mode	Frequency, Hz	Damping ratio
Oxidizer and fuel tanks empty and at standby pressure	1	6.21	0.022
	2	14.20	.024
Oxidizer and fuel tanks empty at nominal flight pressures	1	6.12	0.023
	2	14.51	.053
	3	31.90	.023
	4	37.00	.022
Simulated flight conditions at T + 150 seconds	1	4.93	0.022
	2	9.89	.033
	3	25.71	.014
	4	35.09	No data
Simulated flight conditions at T + 100 seconds	1	3.58	0.025
	2	8.13	.011
	3	17.42	.012
	4	23.12	.009
Simulated flight conditions at T + 75 seconds	1	3.00	0.024
	2	7.77	.013
	3	13.44	.012
	4	20.37	.031
	5	31.44	.002
Simulated conditions at T + 0 (lift-off)	1	2.59	0.019
	2	6.49	.013
	3	9.82	.019
	4	12.74	No data
	5	17.98	0.004

(b) Excitation force in X-Z plane

Test condition	Mode	Frequency, Hz	Damping ratio
Oxidizer and fuel tanks empty at flight pressures	1	6.21	0.037
	2	13.49	.058
	3	31.40	No data
Simulated flight conditions at T + 150 seconds	1	4.74	0.035
	2	10.78	No data
	3	26.62	0.025
	4	36.60	No data
Simulated flight conditions at T + 75 seconds	1	2.97	0.026
	2	8.01	No data
	3	13.35	0.014
	4	20.60	.006
	5	32.89	.016
Simulated conditions at T + 0 (lift-off)	1	2.60	0.023
	2	6.52	.021
	3	10.01	.022
	4	13.01	.026
	5	17.90	.006

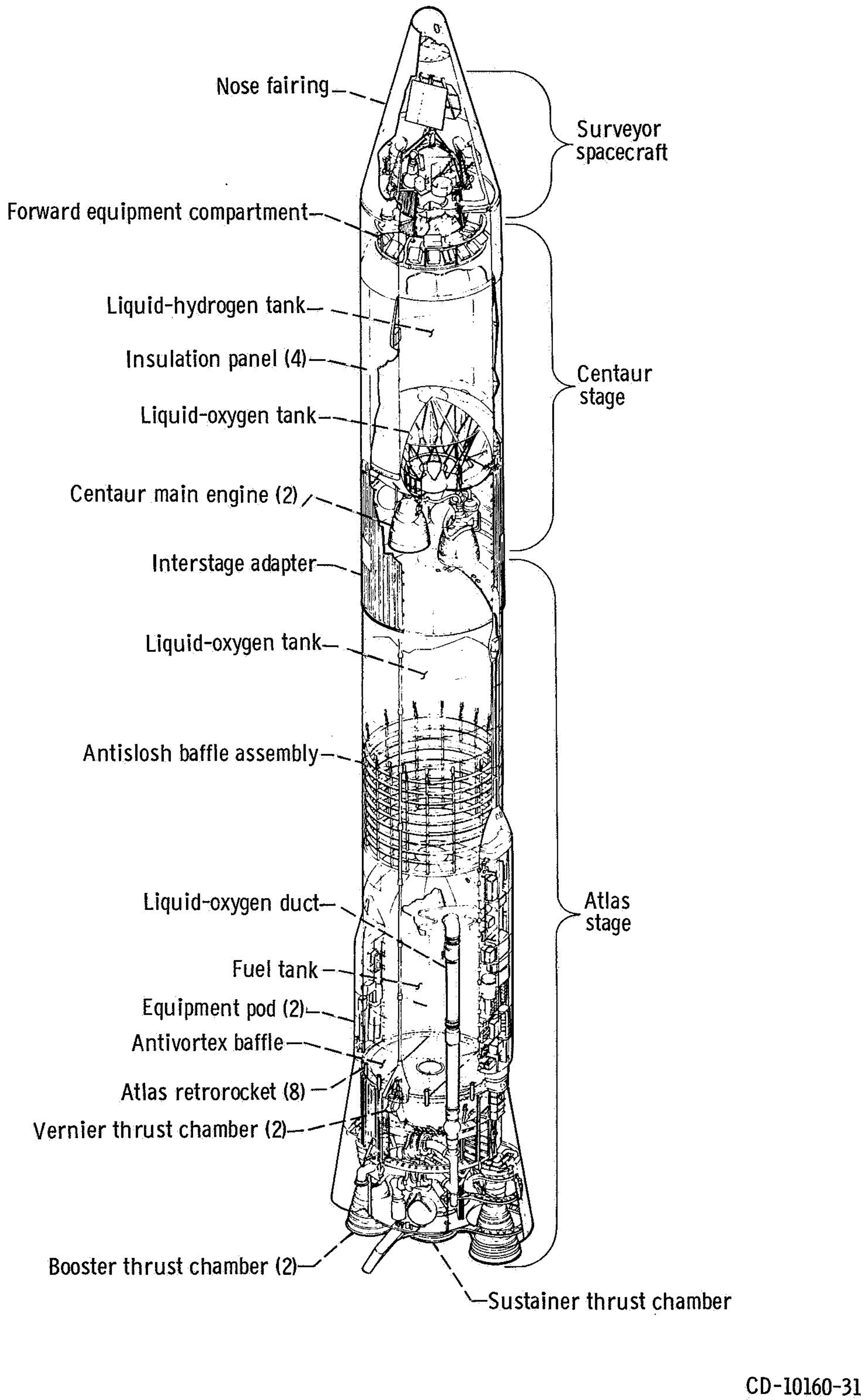

Figure 1. - Atlas-Centaur-Surveyor space vehicle configuration.

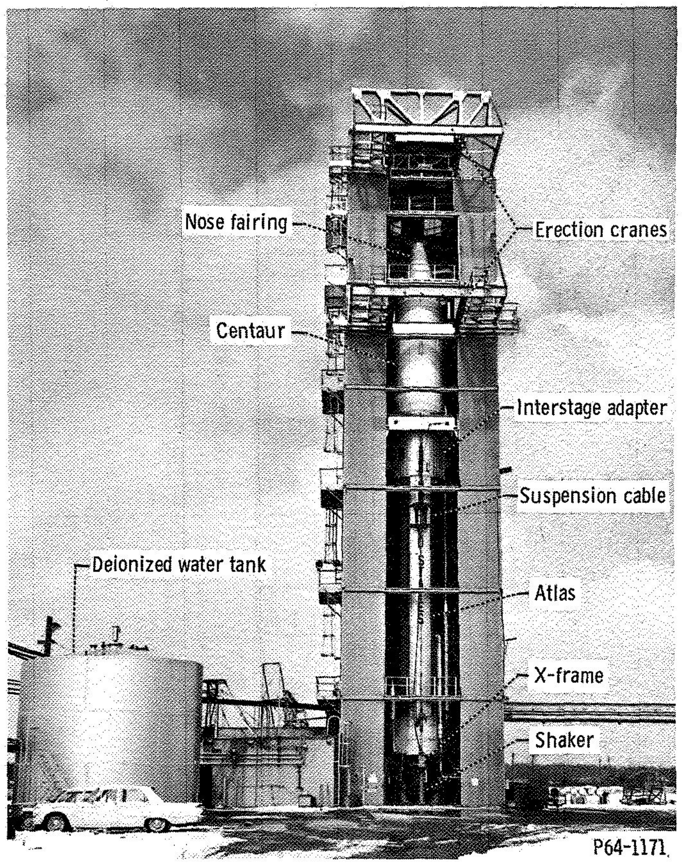

(a) E-stand test facility with Atlas-Centaur-Surveyor.

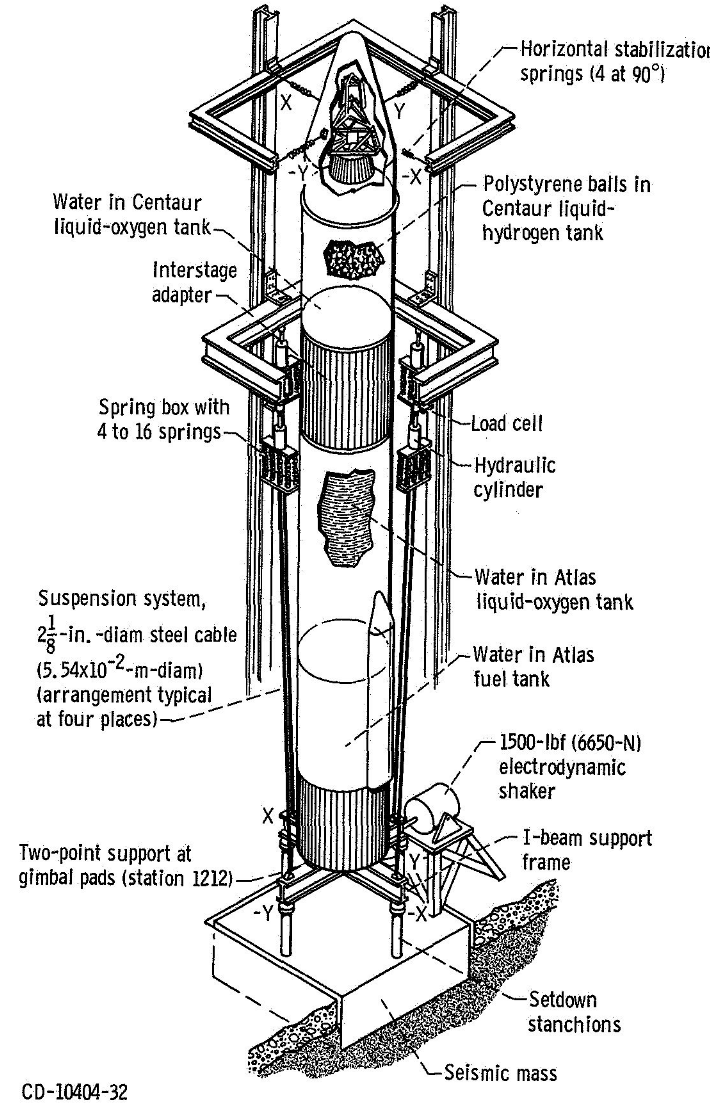

(b) Vehicle support system.

Figure 2. - Test setup.

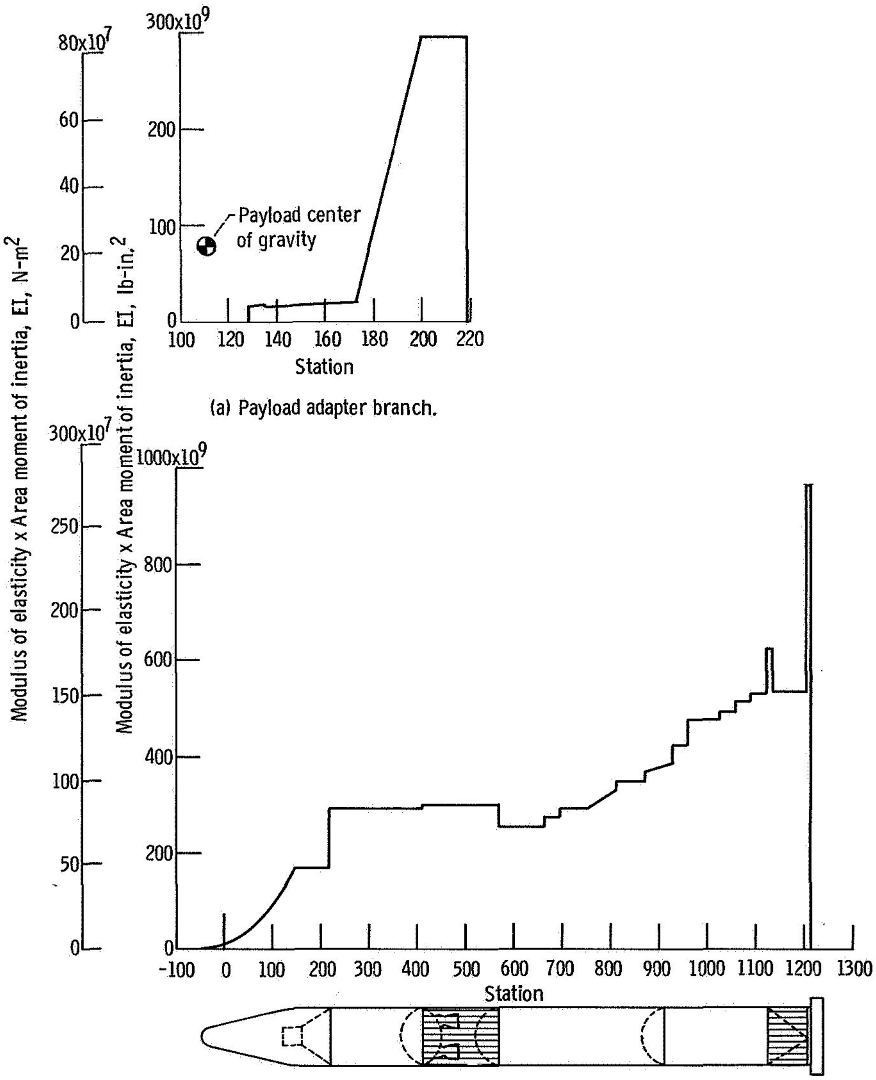

(a) Payload adapter branch.

(b) Entire vehicle.

Figure 3. - Bending stiffness distribution for Plum Brook vehicle.

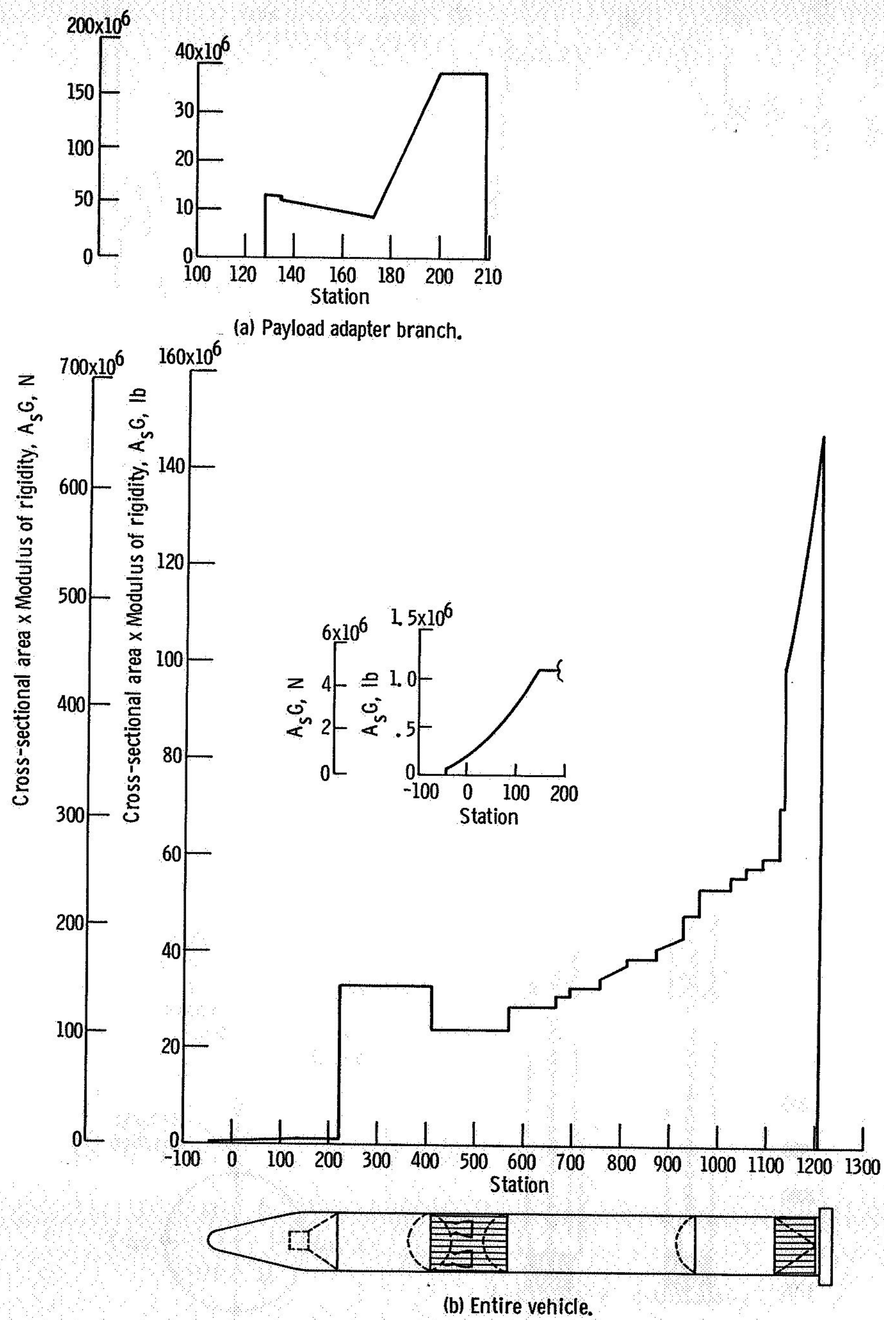

Figure 4. - Shearing stiffness distribution for Plum Brook vehicle.

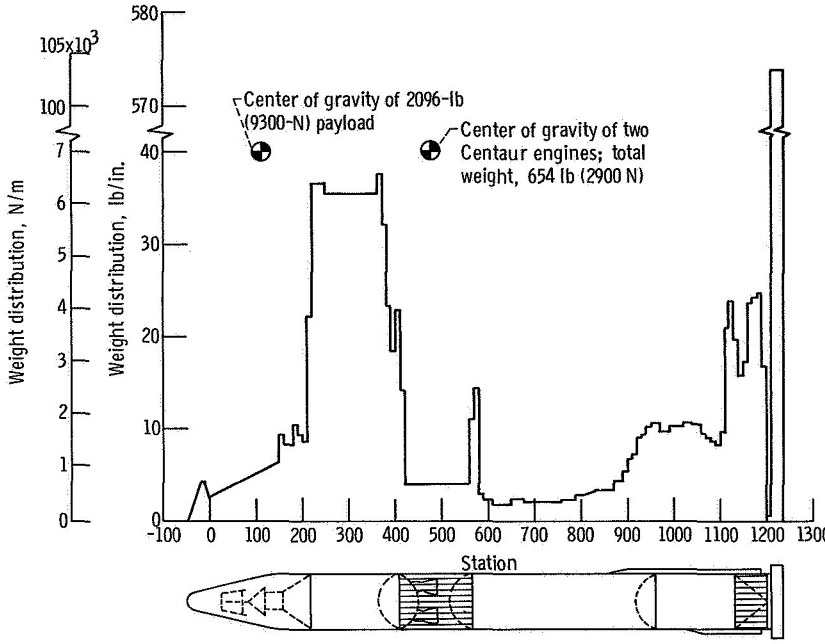

Figure 5. - Weight distribution as function of station for test I configuration.

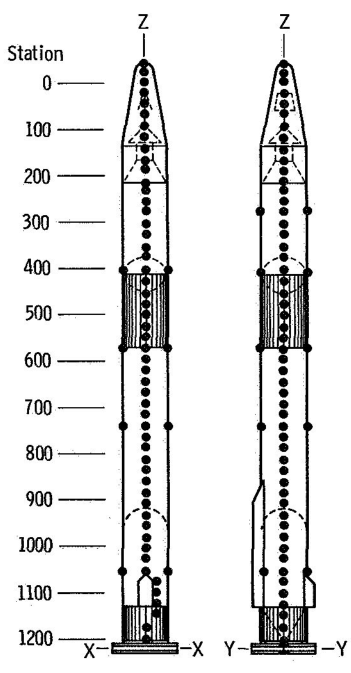

(a) Accelerometer locations for testing in X-Z and Y-Z planes. Each accelerometer reads lateral acceleration in direction of axis on which it is located.

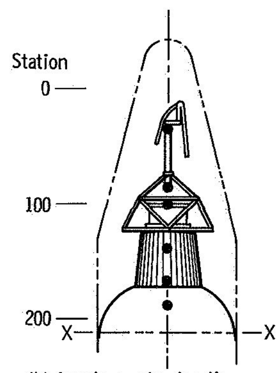

(b) Accelerometer locations on Centaur forward bulkhead, payload adapter, and dynamic Surveyor model. Positions duplicated for testing in Y-Z plane.

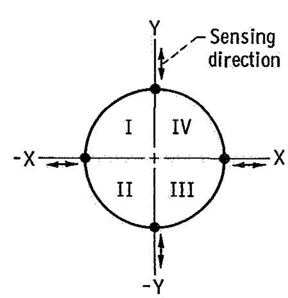

(c) Typical section at stations 1052, 740, 572, 403, and 277.

CD-10407-31

Figure 6. - Location of accelerometers.

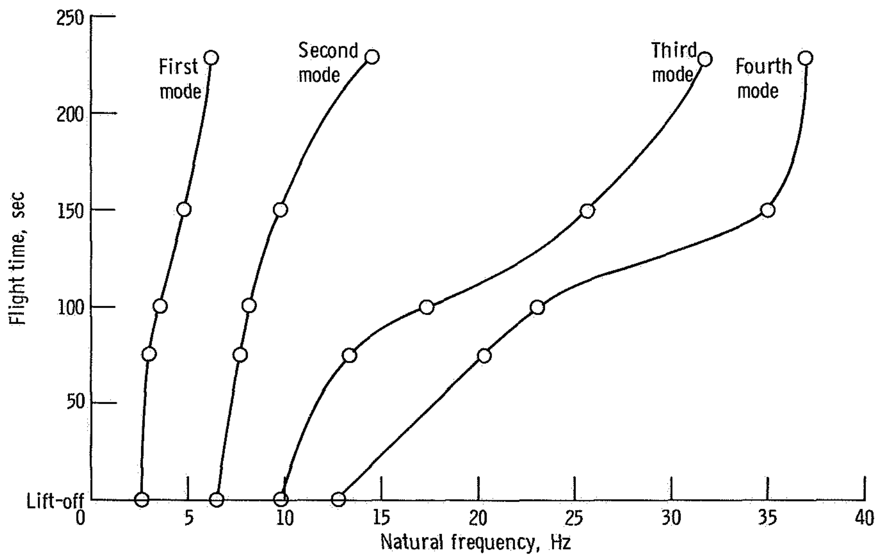

Figure 7. - Variation of natural frequency as function of simulated flight time.

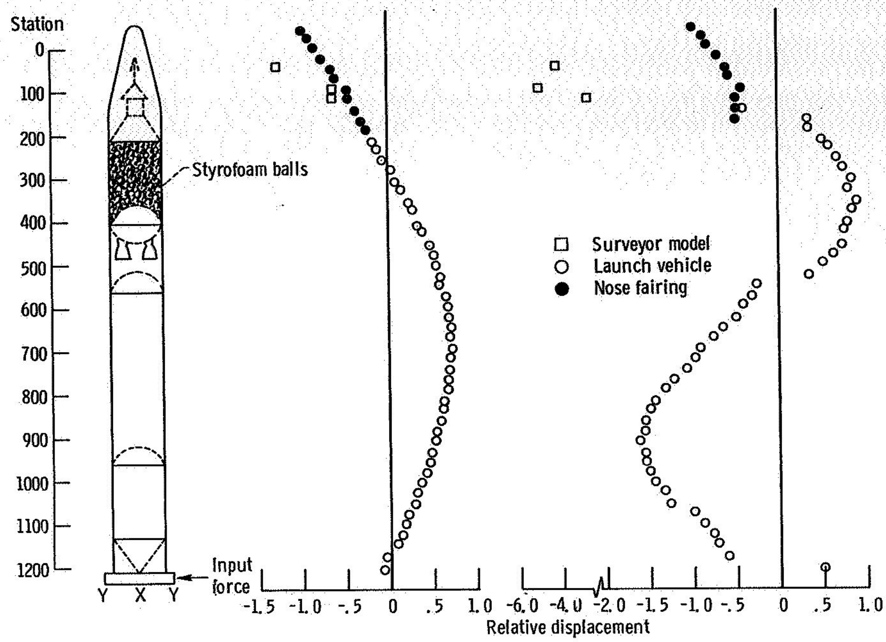

(a-1) First-mode frequency, 5.95 hertz.

(a-2) Second-mode frequency, 14.17 hertz.

(a) Oxidizer and fuel tanks empty at standby pressures (10 and 17 psig (6.89×10^4 and 11.7×10^4 N/m^2 gage), respectively); Y-Z plane.

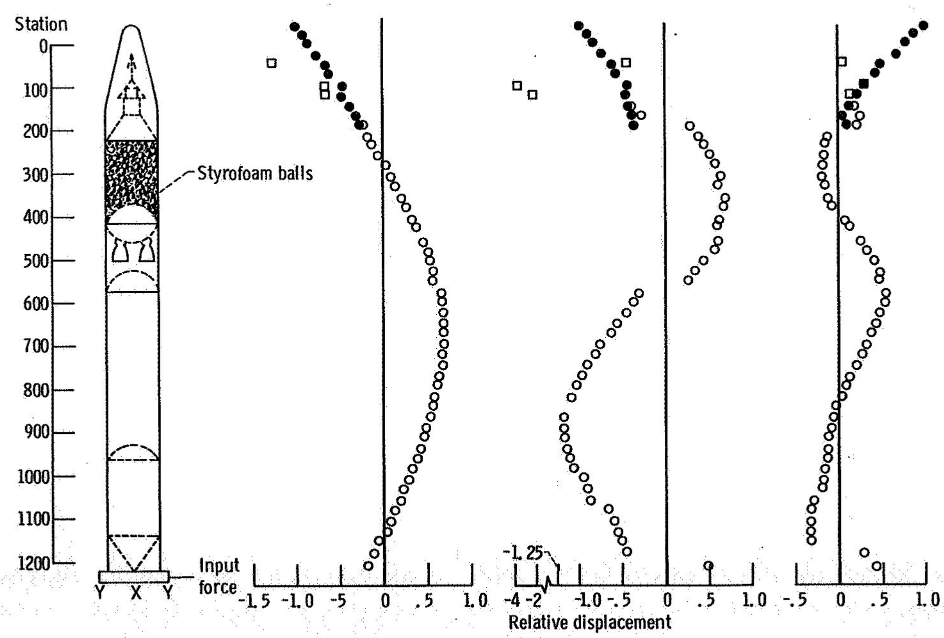

(b-1) First-mode frequency, 6.12 hertz.

(b-2) Second-mode frequency, 14.51 hertz.

(b-3) Third-mode frequency, 31.90 hertz.

(b) Oxidizer and fuel tanks empty at flight pressure; Y-Z plane.

Figure 8. - Lateral dynamics - bending mode shapes. Surveyor dynamic model SD-4.

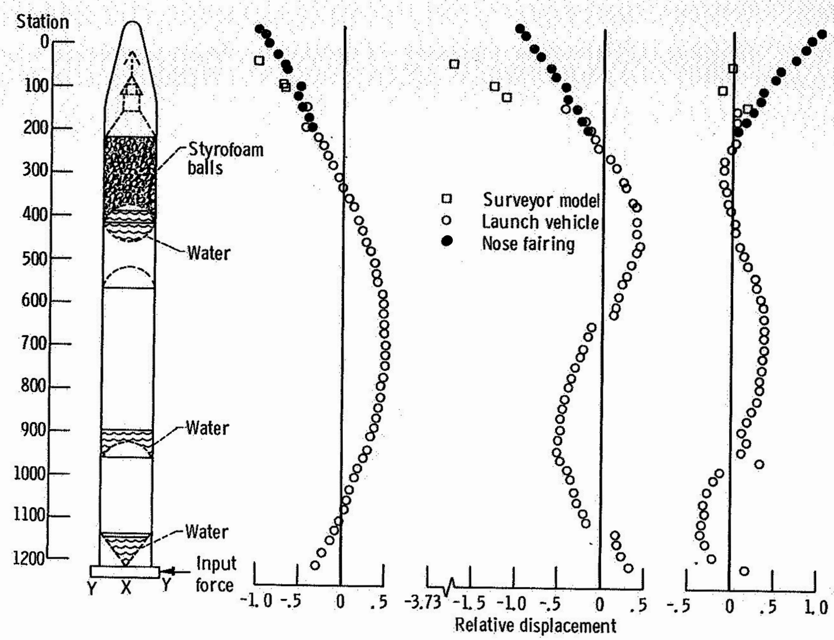

(c-1) First-mode frequency, 4.93 hertz.

(c-2) Second-mode frequency, 9.89 hertz.

(c-3) Third-mode frequency, 25.71 hertz.

(c) Simulated flight conditions at T + 150 seconds; Y-Z plane.

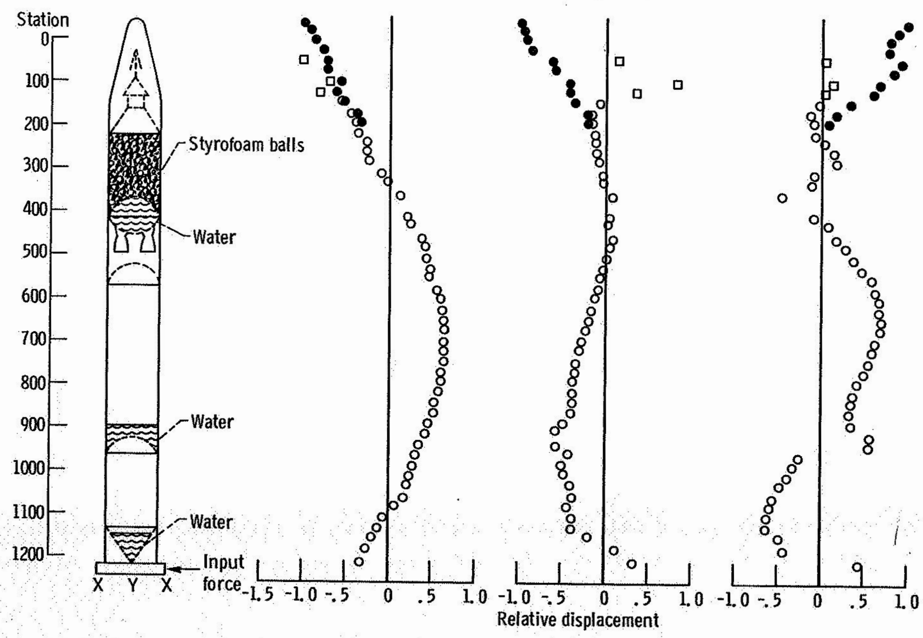

(d-1) First-mode frequency, 4.74 hertz.

(d-2) Second-mode frequency, 17.65 hertz.

(d-3) Third-mode frequency, 26.60 hertz.

(d) Simulated flight conditions at T + 150 seconds; X-Z plane.

Figure 8. - Continued.

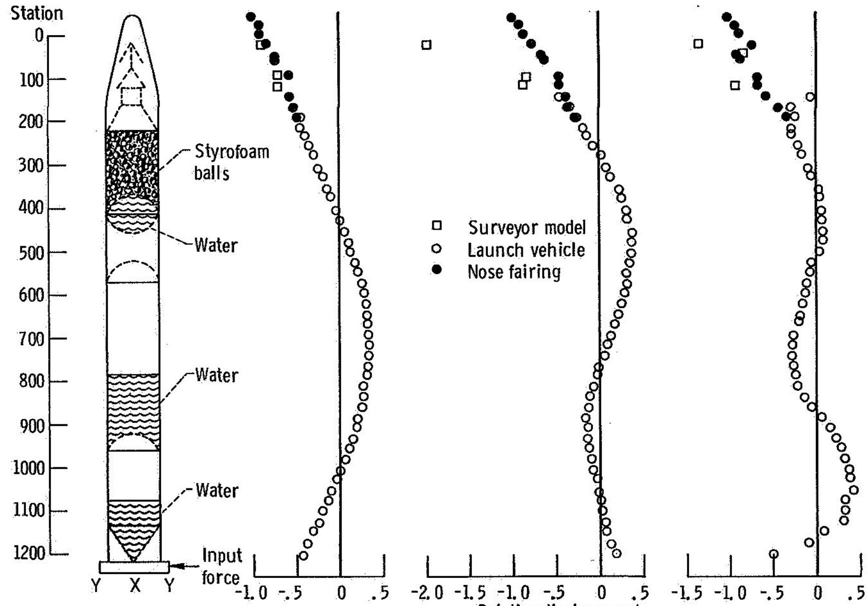

(e-1) First-mode frequency, 3.58 hertz.

(e-2) Second-mode frequency, 8.13 hertz.

(e-3) Third-mode frequency, 17.42 hertz.

(e) Simulated flight conditions at T + 100 seconds; Y-Z plane.

Figure 8. - Continued.

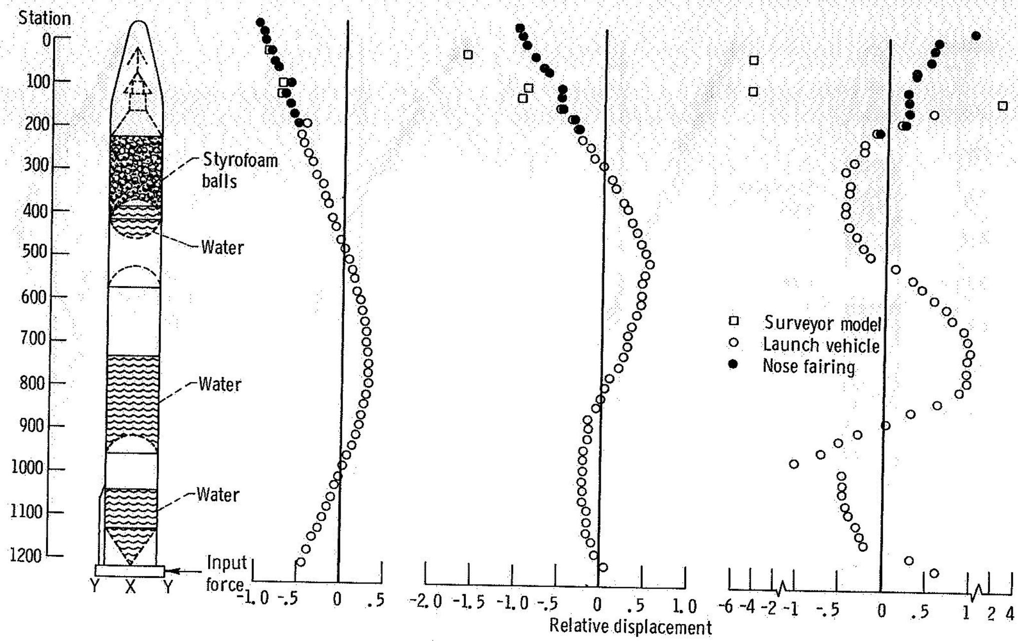

(f-1) First-mode frequency, 3.0 hertz.

(f-2) Second-mode frequency, 7.77 hertz.

(f-3) Third-mode frequency, 13.44 hertz.

(f) Simulated flight conditions at T + 75 seconds; Y-Z plane.

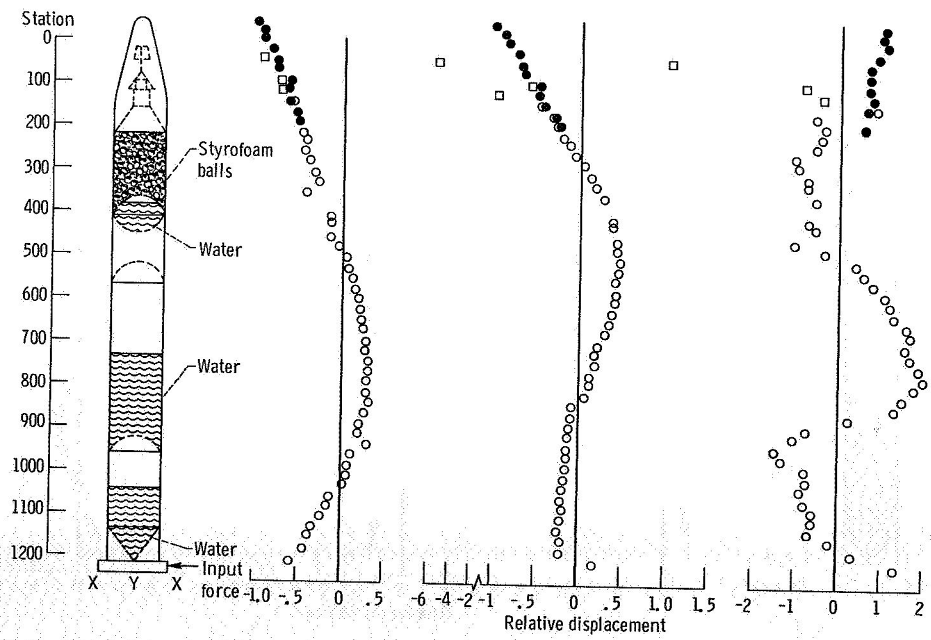

(g-1) First-mode frequency, 2.97 hertz.

(g-2) Second-mode frequency, 8.01 hertz.

(g-3) Third-mode frequency, 13.35 hertz.

(g) Simulated flight conditions at T + 75 seconds; X-Z plane.

Figure 8. - Continued.

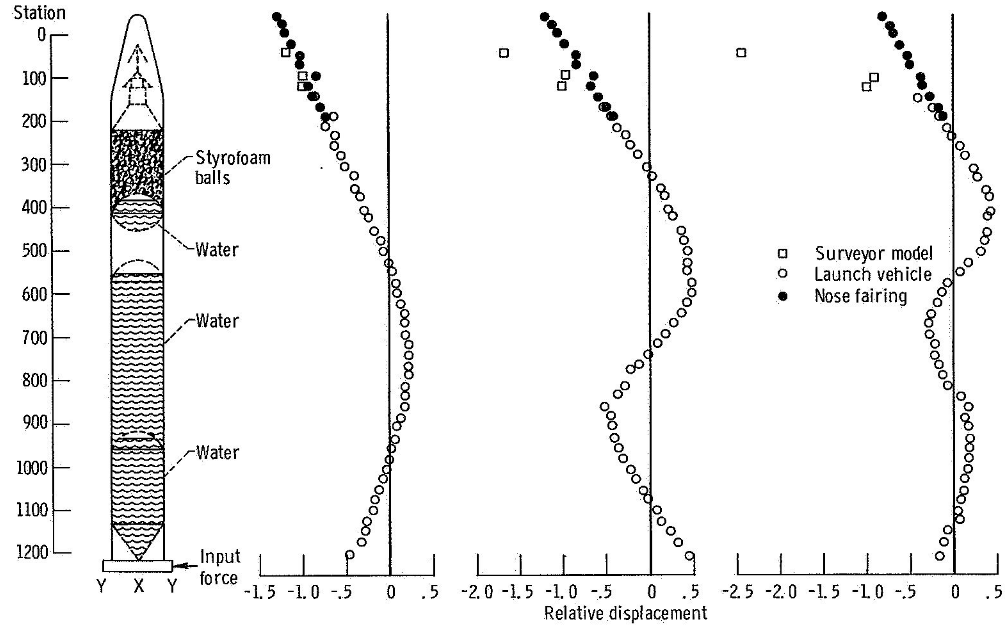

(h-1) First-mode frequency, 2.59 hertz.

(h-2) Second-mode frequency, 6.49 hertz.

(h-3) Third-mode frequency, 9.82 hertz.

(h) Simulated flight conditions at lift-off; Y-Z plane.

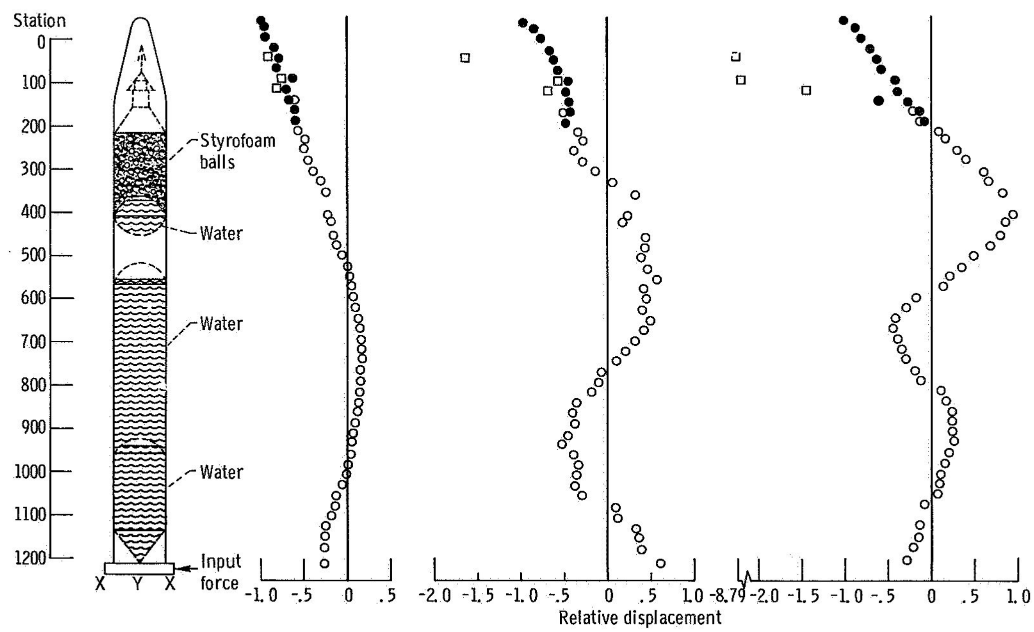

(i-1) First-mode frequency, 2.60 hertz.

(i-2) Second-mode frequency, 6.52 hertz.

(i-3) Third-mode frequency, 10.01 hertz.

(i) Simulated flight conditions at lift-off; X-Z plane.

Figure 8. - Concluded.

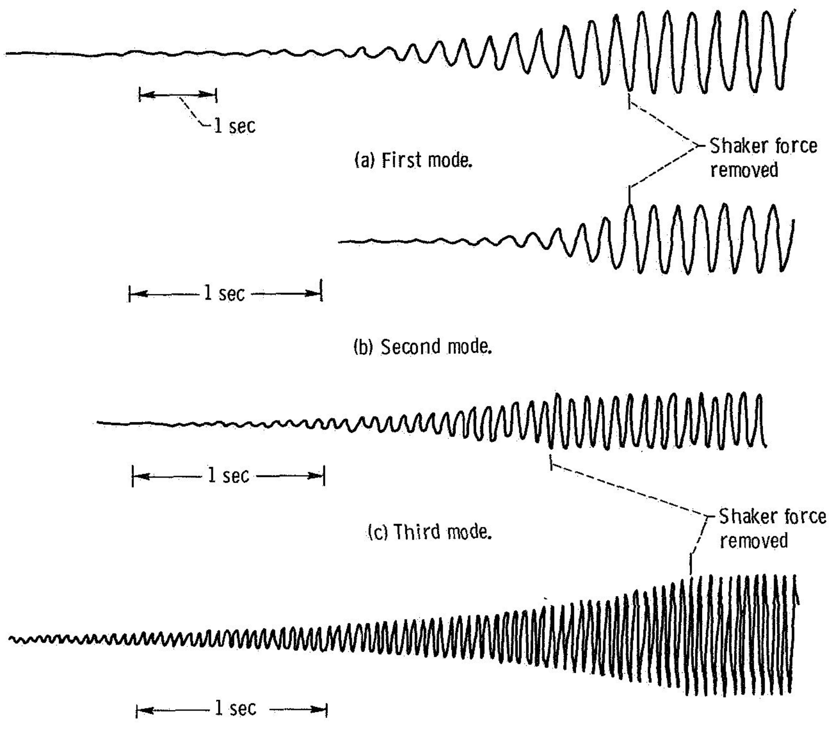

Figure 9. - Typical data used to calculate damping by decay methods in Atlas-Centaur-Surveyor lateral dynamics tests. Simulated flight conditions at T + 75 seconds.

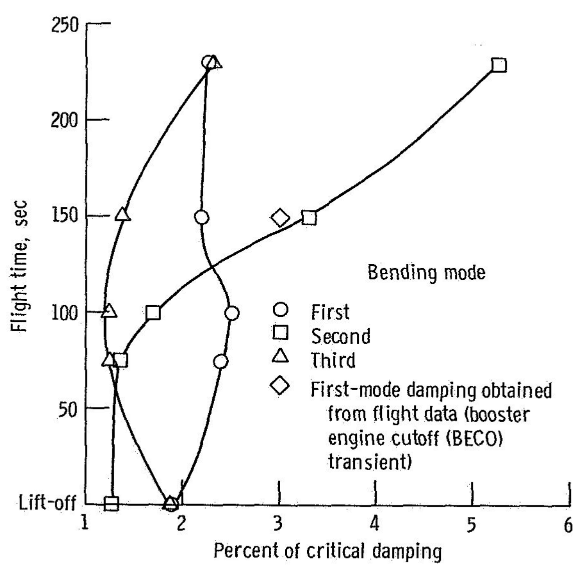

Figure 10. - Percent of critical damping as function of flight time; Y-Z plane (pitch).

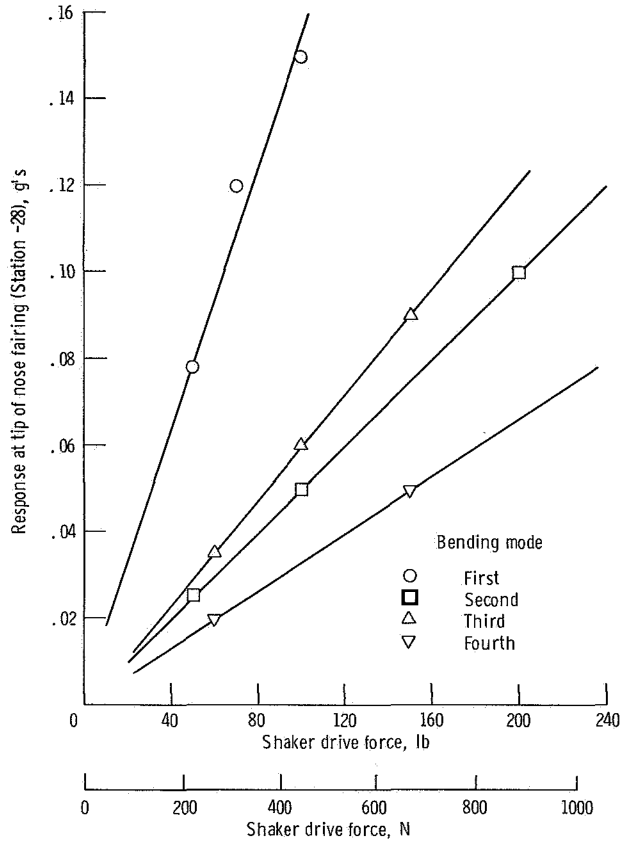

Figure 11. - Response at tip of nose fairing as function of shaker drive force. Simulated flight conditions at T + 75 seconds.

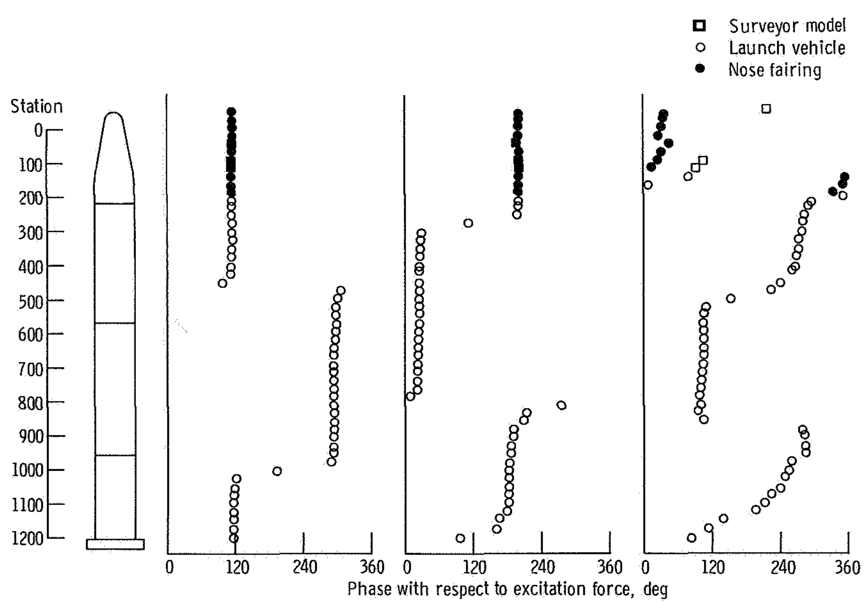

Figure 12. - Phase with respect to excitation force as function of vehicle station. Simulated flight conditions at T + 75 seconds; Y-Z plane.

NASA-Langley, 1969 —— 31 E-4995

NATIONAL AERONAUTICS AND SPACE ADMINISTRATION
WASHINGTON, D. C. 20546

OFFICIAL BUSINESS

FIRST CLASS MAIL

POSTAGE AND FEES PAI
NATIONAL AERONAUTICS
SPACE ADMINISTRATIO

POSTMASTER: If Undeliverable (Section 1
Postal Manual) Do Not Re

"The aeronautical and space activities of the United States shall be conducted so as to contribute . . . to the expansion of human knowledge of phenomena in the atmosphere and space. The Administration shall provide for the widest practicable and appropriate dissemination of information concerning its activities and the results thereof."

— NATIONAL AERONAUTICS AND SPACE ACT OF 1958

NASA SCIENTIFIC AND TECHNICAL PUBLICATIONS

TECHNICAL REPORTS: Scientific and technical information considered important, complete, and a lasting contribution to existing knowledge.

TECHNICAL NOTES: Information less broad in scope but nevertheless of importance as a contribution to existing knowledge.

TECHNICAL MEMORANDUMS: Information receiving limited distribution because of preliminary data, security classification, or other reasons.

CONTRACTOR REPORTS: Scientific and technical information generated under a NASA contract or grant and considered an important contribution to existing knowledge.

TECHNICAL TRANSLATIONS: Information published in a foreign language considered to merit NASA distribution in English.

SPECIAL PUBLICATIONS: Information derived from or of value to NASA activities. Publications include conference proceedings, monographs, data compilations, handbooks, sourcebooks, and special bibliographies.

TECHNOLOGY UTILIZATION PUBLICATIONS: Information on technology used by NASA that may be of particular interest in commercial and other non-aerospace applications. Publications include Tech Briefs, Technology Utilization Reports and Notes, and Technology Surveys.

Details on the availability of these publications may be obtained from:

SCIENTIFIC AND TECHNICAL INFORMATION DIVISION

NATIONAL AERONAUTICS AND SPACE ADMINISTRATION

Washington, D.C. 20546